Supporting Information

Super-Resolution Mapping Reveals NAD$^+$-Delivering Probiotic Extracellular Vesicles as Nanotherapeutics for Organelle Protection and Inflammation Control

Ga-eun Go[1, ‡], Minjae Kang[1, ‡], Bo Kyoung Hwang[2, ‡], Sangoh Choi[1, 3], Uidon Jeong[1], Eunyoung Moon[3], Sang-Hee Lee[3], Seongsu Kang[2], Nae-Gyu Kang[2], Yunkwan Kim[2], Euitaek Jeong[2], Doory Kim[1, 4, 5, 6*]

[1]Department of Chemistry, Hanyang University, Seoul 04763, Republic of Korea

[2]R&D Institute, LG Household & Health Care (LG H&H), Seoul 07795, Republic of Korea

[3]Center for Bio-imaging & Translational Research, Korea Basic Science Institute, Cheongju 28119, Republic of Korea

[4]Research Institute for Convergence of Basic Science, Hanyang University, Seoul 04763, Republic of Korea

[5]Institute of Nano Science and Technology, Hanyang University, Seoul 04763, Republic of Korea

[6]Research Institute for Natural Sciences, Hanyang University, Seoul 04763, Republic of Korea

‡These authors contributed equally.

***Corresponding author: doorykim@hanyang.ac.kr**

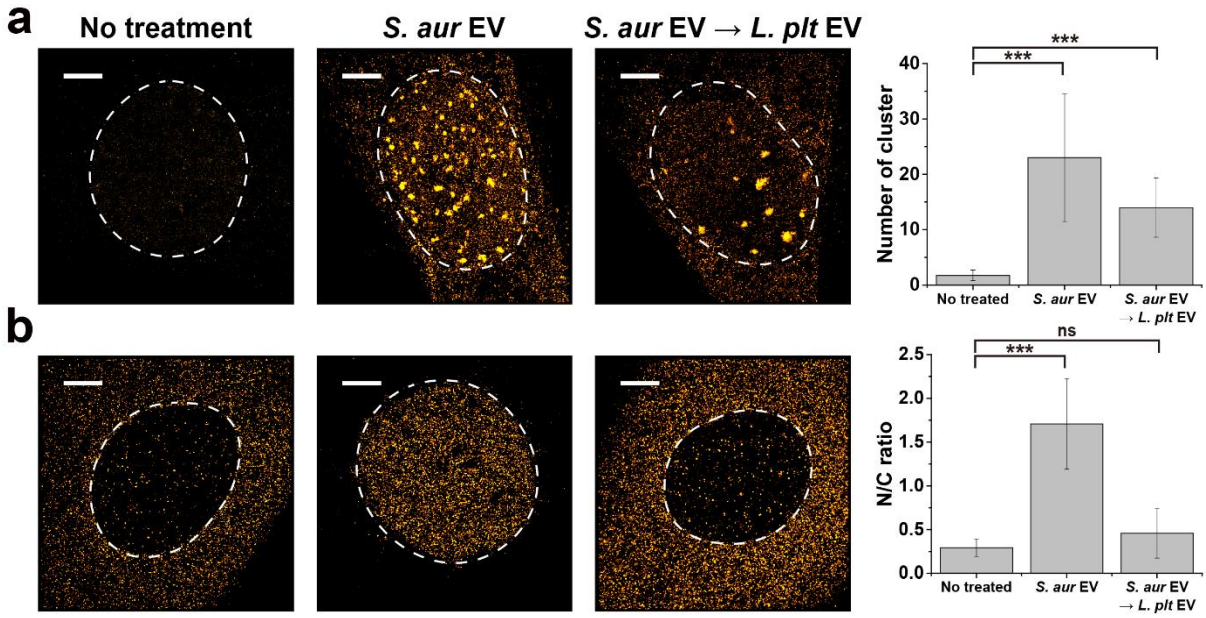

Fig. S1 Representative STORM images of (a) γH2AX and (b) NF-κB in control HDFs, *S. aureus* EV–inflamed cells, and *L. plantarum* EV-treated inflammatory cells. Quantitative analysis of γH2AX foci number in the nucleus and NF-κB nuclear translocation, expressed as the ratio of nuclear to cytosolic localizations, is shown on the right. Scale bars = 5 μm. White dashed line: nucleus boundary. (n = 5; data are represented as mean ± SD) (Two-tailed Student's *t*-test, ns: $p > 0.05$, ***$p < 0.001$)

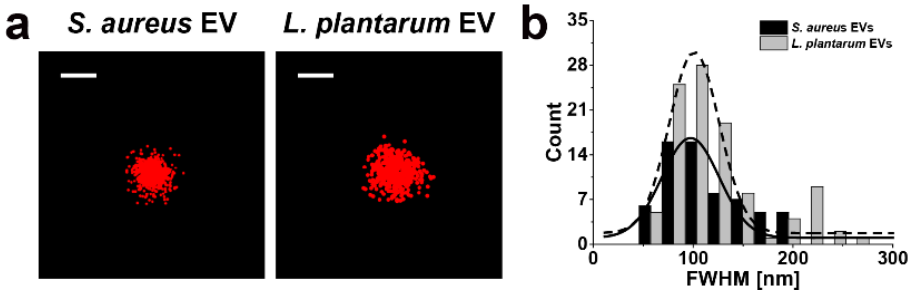

Fig. S2 Representative STORM images of purified EVs from *S. aureus* and *L. plantarum*. (**a**) Representative STORM images of purified EVs labeled with Nile red from *S. aureus* (left) and *L. plantarum* (right). Scale bars = 100 nm. (**b**) Size of EVs measured using STORM images of Nile red-stained purified EV samples.

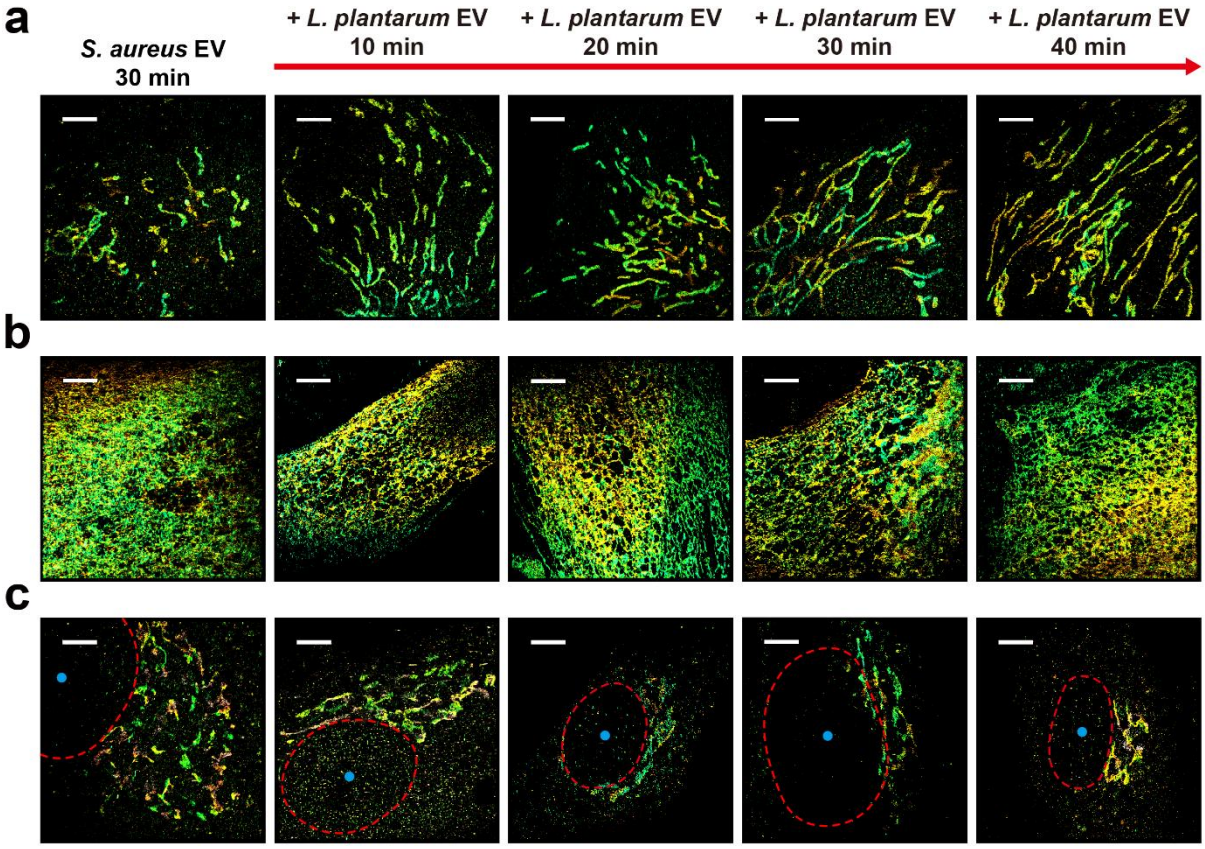

Fig. S3 Representative STORM images showing organelle ultrastructural changes in response to different *L. plantarum* EV-treatment durations in *S. aureus* EV-induced inflammatory cells. (**a**) Effect of varying *L. plantarum* EV exposure times (0, 10, 20, 30, and 40 min) on mitochondrial morphology. (**b**) Impact of *L. plantarum* EV-treatment duration on ER architecture. (**c**) Golgi apparatus reorganization under different *L. plantarum* EV-treatment periods. Red dashed line: nucleus boundary. Scale bars = 5 μm. Quantitative analyses of these ultrastructural changes are presented in Fig. 1D.

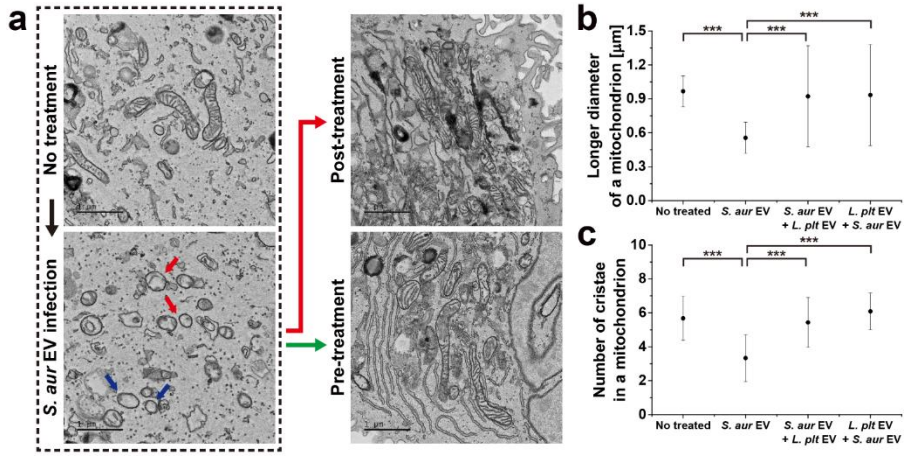

Fig. S4 TEM images showing the restorative effects of *L. plantarum* EVs on host cells. (**a**) Representative TEM images of HDFs showing the restorative effects of *L. plantarum* EVs (6.75×10^7 particles/mL, 30 min) on *S. aureus* EV-induced mitochondrial alterations (6.75×10^7 particles/mL, 30 min), compared with control cells. Both pre- and post-treatment with *L. plantarum* EVs are presented. Red arrows: mitochondrial fission. Blue arrows: cristae loss. Scale bars = 1 μm. (**b**) Quantitative analysis of mitochondrial size in terms of the longer diameter from TEM images. (**c**) Quantitative analysis of the number of cristae in a mitochondrion from TEM images. (n = 10; data are represented as mean ± SD) (***$p < 0.001$)

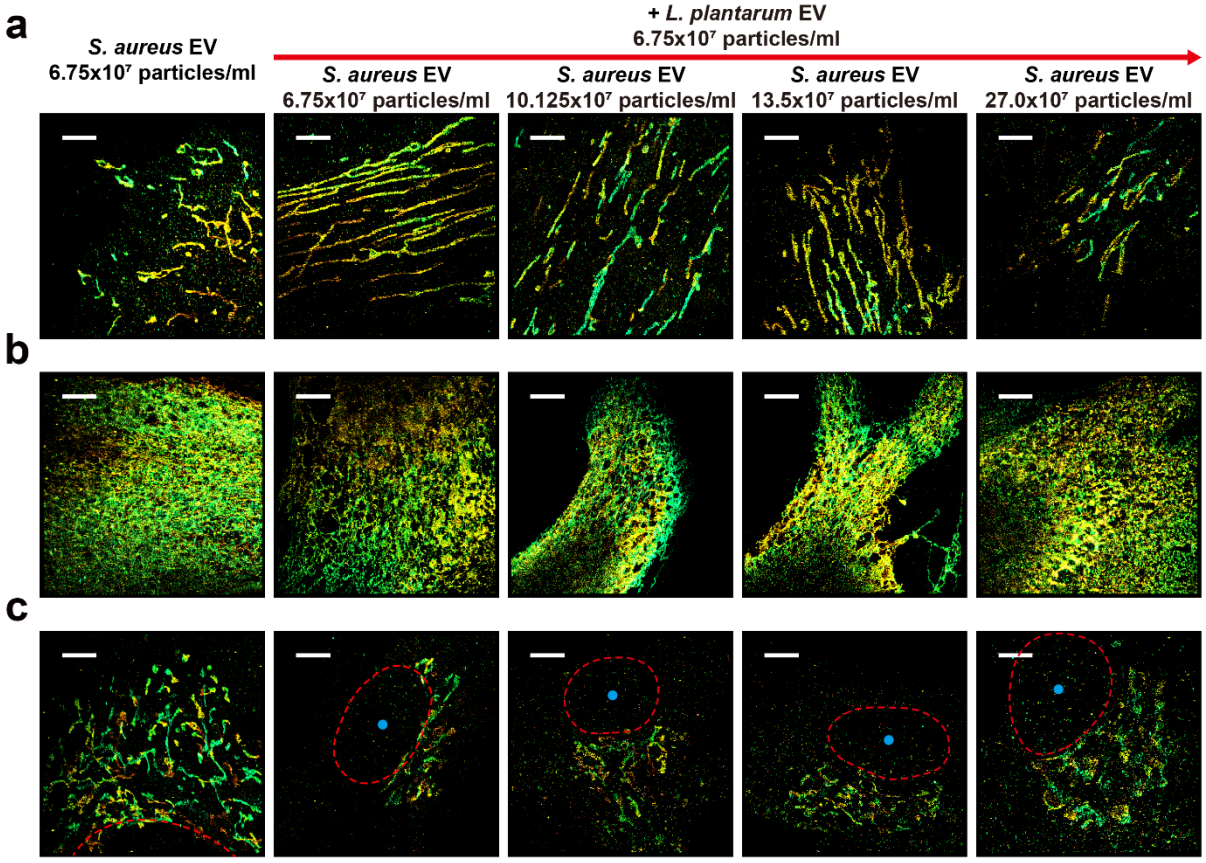

Fig. S5 Representative STORM images showing organelle ultrastructural alterations in response to *L. plantarum* EV-treatment across different inflammatory states established by varying *S. aureus* EV concentrations. (**a**) Mitochondrial morphological changes following *L. plantarum* EV-treatment in cells pre-exposed to different *S. aureus* EV concentrations. (**b**) ER structural modifications after *L. plantarum* EV-treatment in cells with different inflammatory baselines created by varying *S. aureus* EV concentrations. (**c**) Golgi apparatus reorganization in response to *L. plantarum* EV-treatment across distinct inflammatory conditions established by different *S. aureus* EV concentrations. Red dashed line: nucleus boundary. Scale bars = 5 μm. Quantitative analyses of these ultrastructural changes are presented in Fig. 1E.

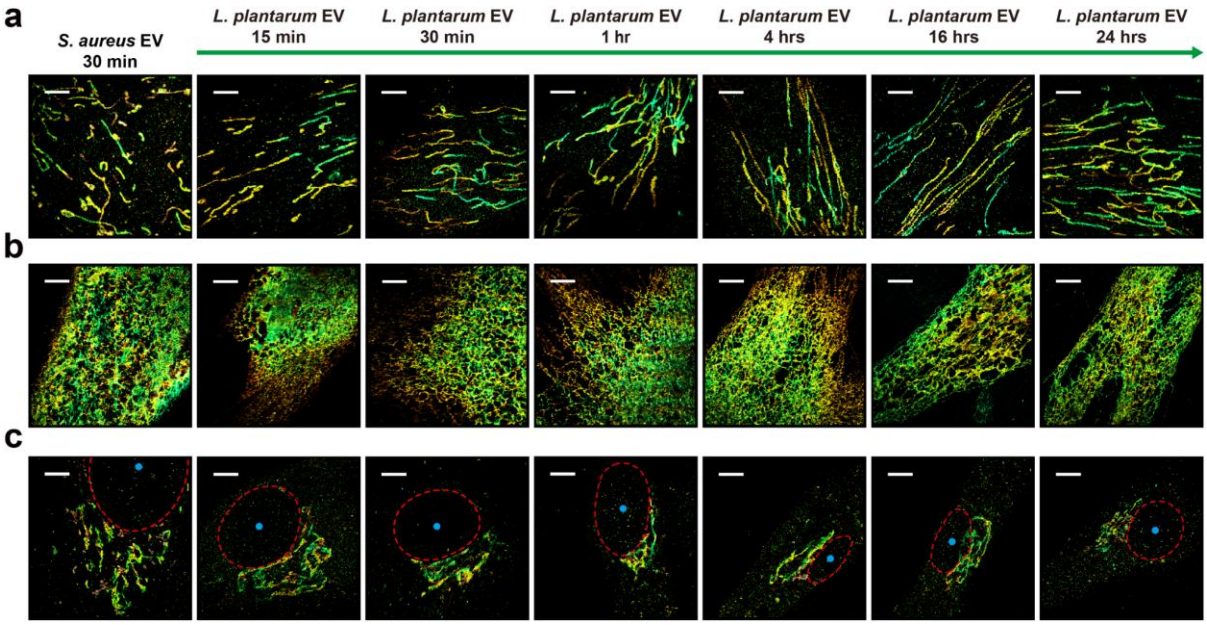

Fig. S6 Representative STORM images showing organelle ultrastructural preservation in response to different *L. plantarum* EV-pretreatment durations prior to *S. aureus* EV exposure. (**a**) Effect of varying *L. plantarum* EV-pretreatment times (0, 0.25, 0.5, 1, 4, 16, and 24 h) on mitochondrial morphology following *S. aureus* EV challenge. (**b**) Impact of *L. plantarum* EV-pretreatment duration on ER network architecture prior to *S. aureus* EV-induced stress. (**c**) Golgi apparatus organization under different *L. plantarum* EV-pretreatment periods prior to *S. aureus* EV exposure. Red dashed line: nucleus boundary. Scale bars = 5 μm. Quantitative analyses of these ultrastructural changes are presented in Fig. 2D.

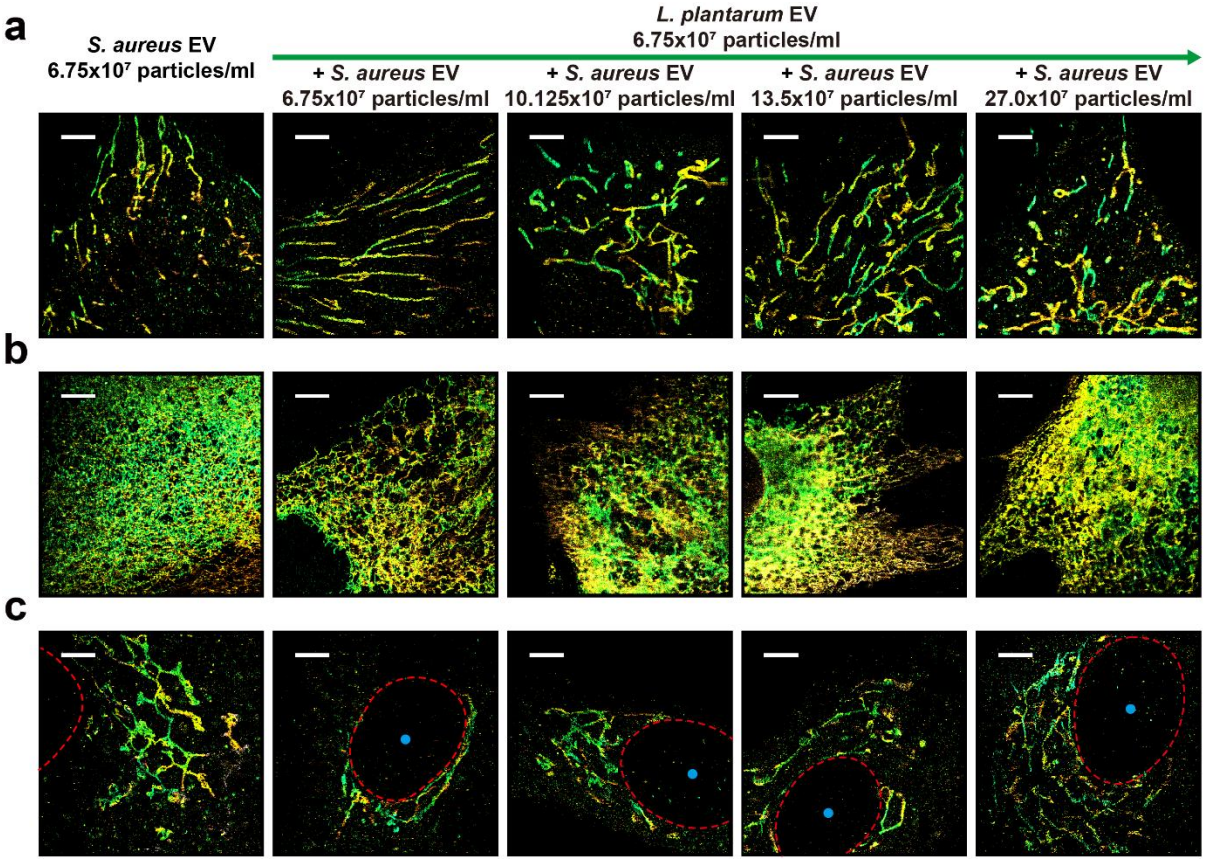

Fig. S7 Representative STORM images showing organelle ultrastructural preservation in response to *L. plantarum* EV-pretreatment across different inflammatory challenges, established by varying *S. aureus* EV concentrations. (**a**) Mitochondrial morphological changes in *L. plantarum* EV-pretreated cells exposed to different *S. aureus* EV concentrations. (**b**) ER structural modifications in *L. plantarum* EV-pretreated cells challenged with different *S. aureus* EV concentrations. (**c**) Golgi apparatus organization in *L. plantarum* EV-pretreated cells under varying inflammatory conditions induced by different *S. aureus* EV concentrations. Red dashed line: nucleus boundary. Scale bars = 5 μm. Quantitative analyses of these ultrastructural changes are presented in Fig. 2E.

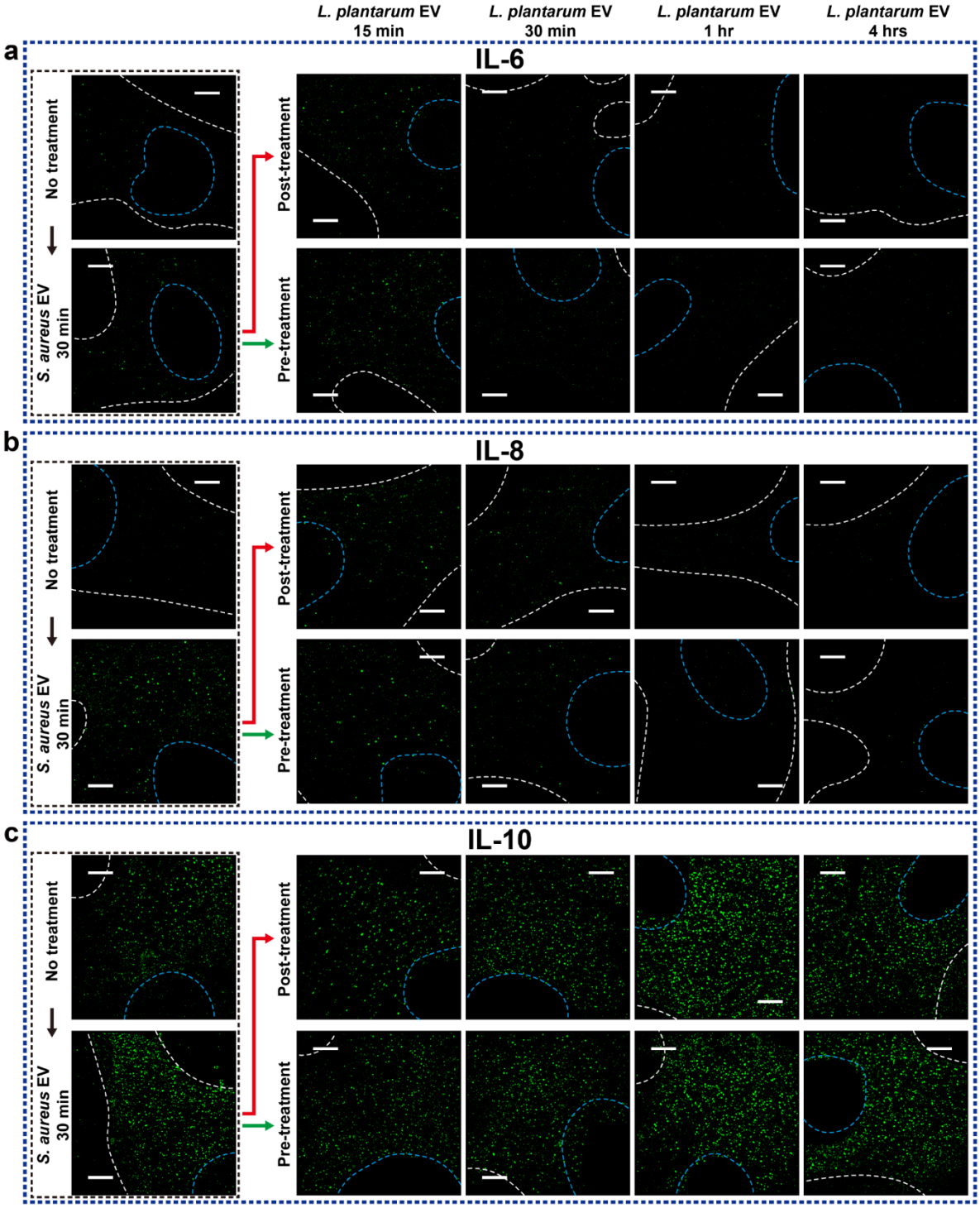

Fig. S8 Representative STORM images of intracellular cytokine clustering. (**a**) IL-6, (**b**) IL-8, and (**c**) IL-10 under different treatment conditions. For each cytokine, panels show untreated control cells, cells treated with *S. aureus* EVs (6.75×10^7 particles/mL, 30 min), and cells pre-treated (bottom row) or post-treated (top row) with *L. plantarum* EVs, at the indicated time intervals. Blue dashed line: nucleus boundary. White dashed line: cell boundary. Scale bars = 5 μm. Quantitative analyses of these ultrastructural changes are presented in Fig. 3D.

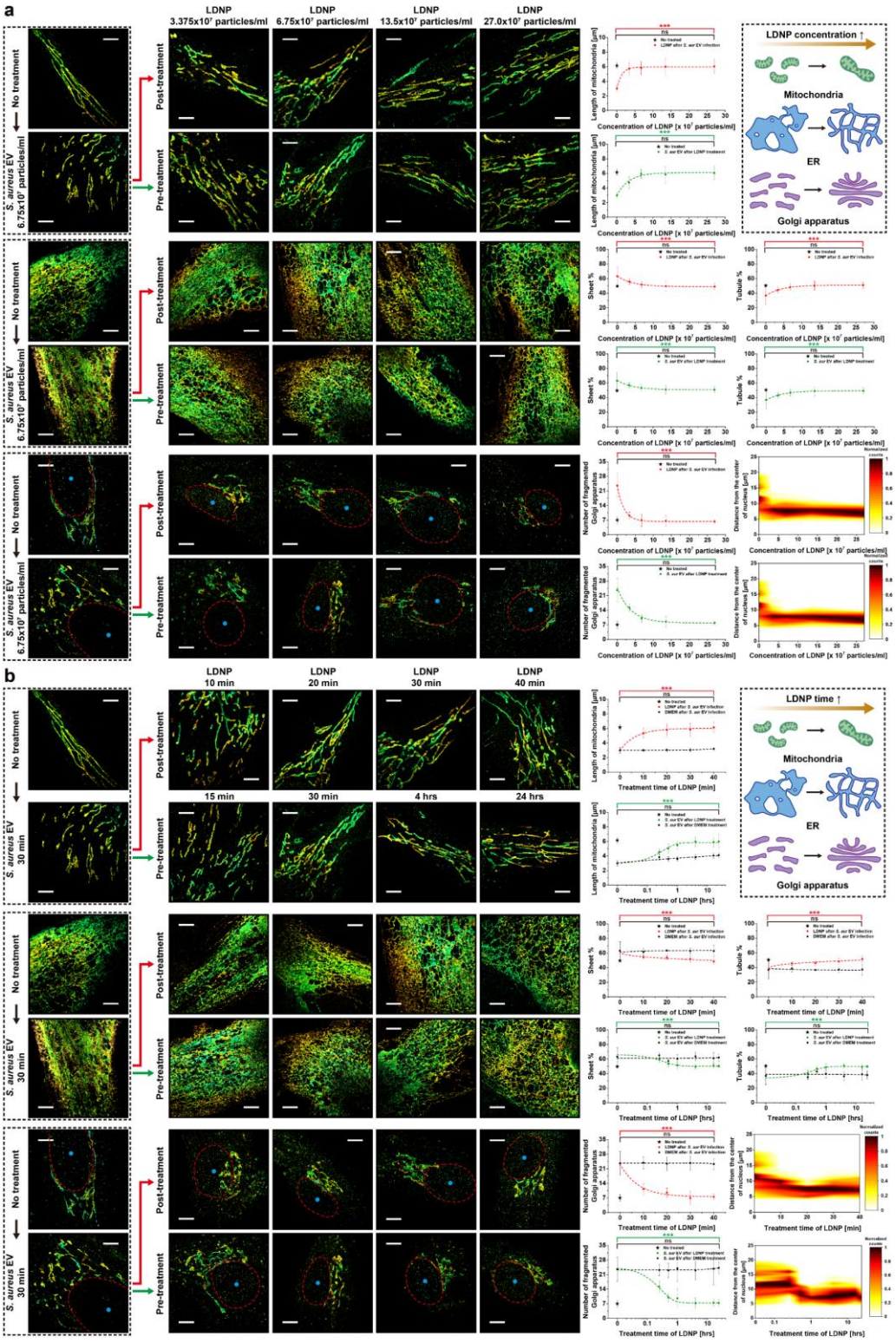

Fig. S9 Representative STORM images and quantification of mitochondria (top), ER (middle), and Golgi (bottom) as a function of LDNP treatment concentration (**a**) and duration (**b**) measured using STORM images. Post-treatment values are shown as red curves, pre-treatment values as green curves, and control values (DMEM-treated) as black curves. Red dashed line: nucleus boundary. Scale bars = 5 μm. (n = 8; data are represented as mean ± SD) (ns: $p > 0.05$, ***$p < 0.001$)

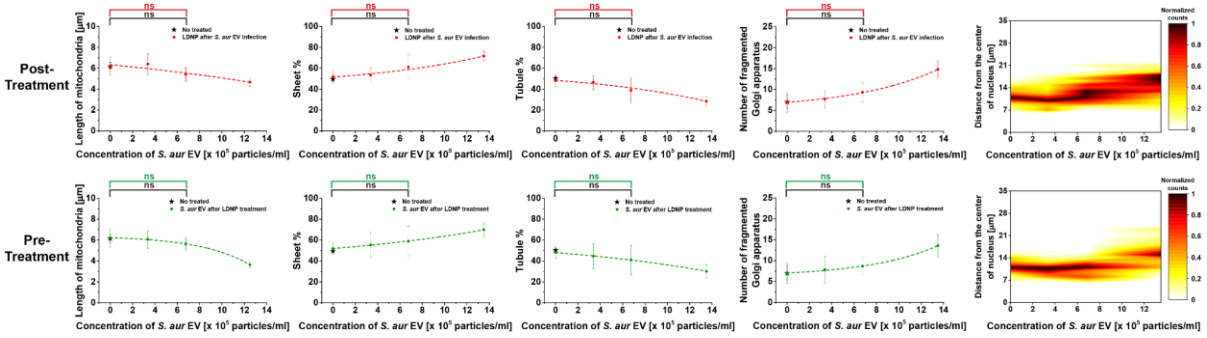

Fig. S10 STORM quantitative imaging analysis of organelle ultrastructural alterations in response to treatment with 6.75×10^5 particles/mL of LDNPs across different inflammatory states, established by varying *S. aureus* EV concentrations. (n = 8; data are represented as mean ± SD) (ns: $p > 0.05$)

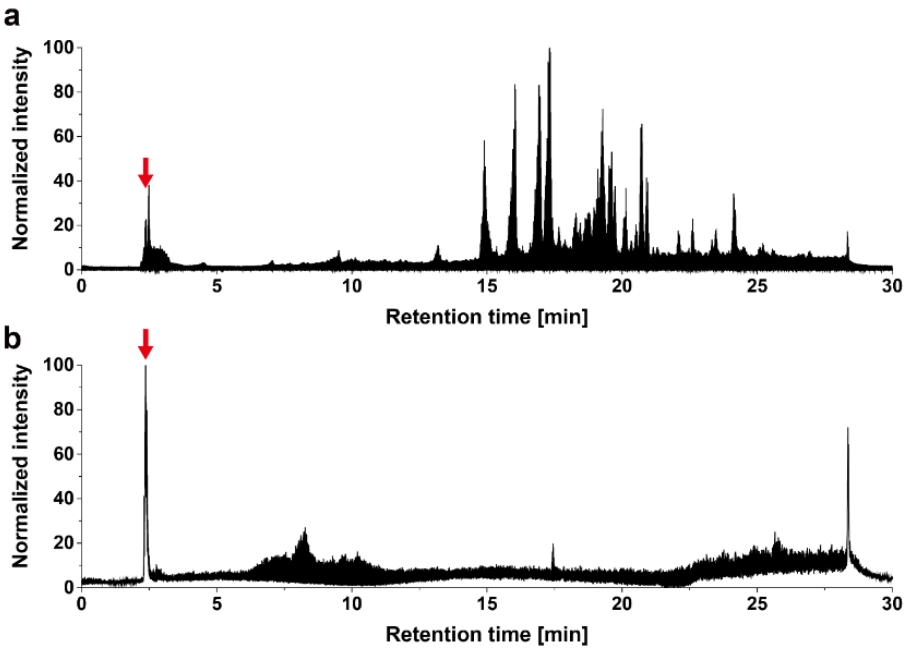

Fig. S11 LC–MS chromatograms of (**a**) *L. plantarum* EVs and (**b**) NAD^+ standard. In both chromatograms, the peak corresponding to NAD^+ is indicated by a red arrow, with the EV sample a showing an identical retention time to that of the NAD^+ standard (**b**).

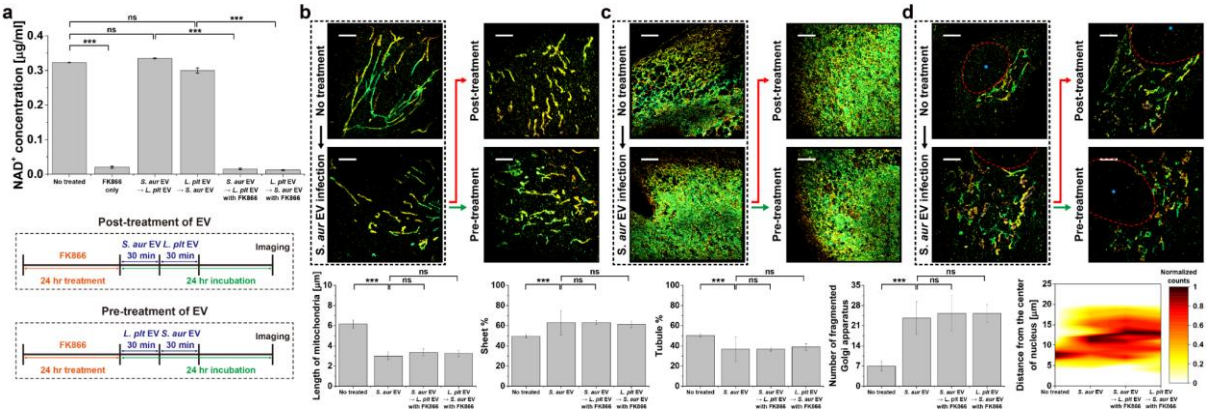

Fig. S12 The effect of the NAD^+ inhibitor FK866 on the organelle-restorative activity of *L. plantarum* EVs in host cells. (a) Quantification of intracellular NAD^+ levels in untreated control cells and *S. aureus* EV–infected cells following either pre-treatment (30 min) or post-treatment (30 min) with *L. plantarum* EVs, in the presence or absence of the NAD^+ inhibitor FK866. (b-d) Representative STORM images (top) and quantitative analyses (bottom) of (b) mitochondria, (c) endoplasmic reticulum (ER), and (d) Golgi apparatus illustrating the effect of the NAD^+ inhibitor FK866 on the organelle-restorative activity of *L. plantarum* EVs in host cells. Scale bars = 5 μm. (n = 6; data are represented as mean ± SD) (ns: $p > 0.05$, ***$p < 0.001$)

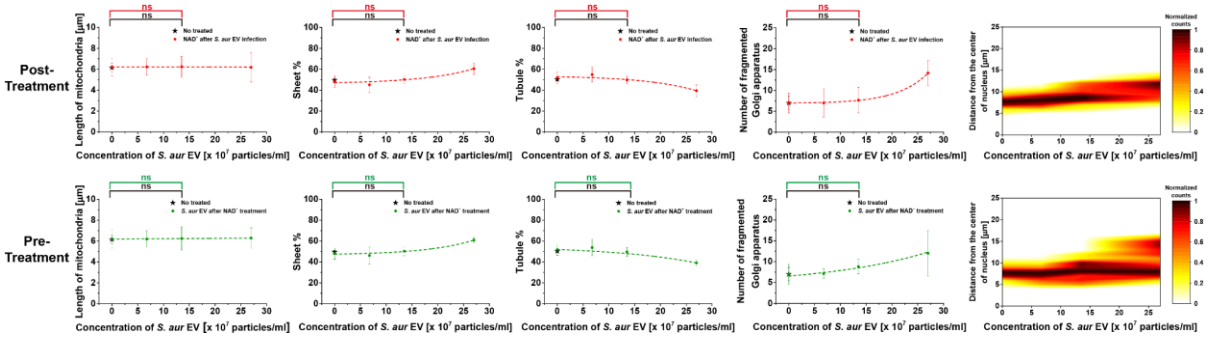

Fig. S13 STORM quantitative imaging analysis of organelle ultrastructural alterations in response to 9.8 μg/mL of NAD^+ treatment across different inflammatory states, established by varying *S. aureus* EV concentrations. (n = 8; data are represented as mean ± SD) (ns: $p > 0.05$)